Interfacing Neural Cells with Typical Microelectronics Materials for Future Manufacturing

Fernando Pesantez Torres[a], Natalya Tokranova[a], Eleanor Amodeo[a], Taylor Bertucci[b], Thomas R. Kiehl[b], Yubing Xie[a], Nathaniel C. Cady[a], Susan T. Sharfstein[a*]

[a] Department of Nanoscale Science and Engineering, College of Nanotechnology, Science and Engineering, University at Albany, State University of New York, 257 Fuller Road, Albany, NY 12203, USA

[b] Neural Stem Cell Institute, One Discovery Drive, Rensselaer, NY 12144, USA

[*] Corresponding author
Susan T. Sharfstein, Ph.D., Professor, Department of Nanoscale Science and Engineering, University at Albany, 257 Fuller Road, Albany, NY 12203, USA
Phone: 518-437-8820
Fax: 518-437-8687
Email: ssharfstein@albany.edu

Abstract

The biocompatibility of materials used in electronic devices is critical for the development of implantable devices like pacemakers and neuroprosthetics, as well as in future biomanufacturing. Biocompatibility refers to the ability of these materials to interact with living cells and tissues without causing an adverse response. Therefore, it is essential to evaluate the biocompatibility of metals and semiconductor materials used in electronic devices to ensure their safe use in medical applications. Here, we evaluated the biocompatibility of a collection of diced silicon chips coated with a variety of metal thin films, interfacing them with different cell types, including murine mastocytoma cells in suspension culture, adherent NIH 3T3 fibroblasts, and human induced pluripotent stem cell (iPSC)-derived neural progenitor cells (NPCs). All materials tested were biocompatible and showed the potential to support neural differentiation of iPSC-NPCs, creating an opportunity to use these materials in a scalable production of a range of biohybrid devices such as electronic devices to study neural behaviors and neuropathies.

Keywords: Biocompatibility; Semiconductor materials; Metal-cell interaction; Pluripotent stem cells; Neural cells; Biomanufacturing.

1. Introduction

Scientists, engineers, and physicians have expanded their focus on the construction of effective interfaces between living cells and electronic and photonic devices (Ahnood et al., 2023; Sharfstein, 2022). Because they facilitate direct contact between biological systems and electronic equipment, biohybrid electronic devices have the potential to revolutionize how we think about biotechnology and biosensing. Scientists and engineers collaborate to create new types of devices that can monitor cellular activities in real-time, detect disease biomarkers, and even control cellular behavior by fusing cells with conventional semiconductor materials. A variety of bioelectronic devices are already used in a wide range of medical applications. Examples include cardiac pacemakers, which celebrated their 50th anniversary in 2013 (Beck et al., 2010), cochlear implants (Clark, 2006; Wilson and Dorman, 2008), neural stimulators to treat for epilepsy or paralysis (Fattahi et al., 2014), deep-brain stimulators (Gimsa et al., 2005; Perlmutter and Mink, 2006), and retinal prosthetic devices for vision loss (Yue et al., 2016). A complete understanding of the behaviors of cells and devices during interactions is essential.

Biocompatibility is commonly defined as a biomaterial's or medical device's ability to perform with an adequate host reaction in a certain application. A bioresponse or biocompatibility assessment (i.e., a biological reaction evaluation) is thought to be a measure of the degree and duration of the detrimental changes in homeostatic systems that govern the host response (Anderson, 2019). Biocompatibility is a critical feature required for biodevices; however, biocompatibility is not necessarily generalizable, and a biomaterial might evoke different responses based on cell type and microenvironment. Tests that are typically used to examine cell proliferation, viability, and cytotoxicity include the alamarBlue assay, mitochondrial dehydrogenase performance measurement such as MTT ((4,5-dimethyl-2-thiazolyl)-2,5-diphenyl-2H-tetrazolium bromide or

methyl thiazolyl tetrazolium assay, XTT (2,3-bis-(2-methoxy-4-nitro-5-sulfophenyl)-2H-tetrazolium-5-carboxanilide) assay, and lactate dehydrogenase (LDH) cytotoxicity assay (LI et al., 2015; Roehm et al., 1991; Salerno et al., 2009; Wang et al., 2013). These tests assess the number of living cells by the metabolic activity of cells (e.g., alamarBlue, MTT, XTT, assay) or cell death by cell membrane damage (e.g., LDH assay).

Interfacing neuronal cells with semiconductor/electronic devices is one of the most promising areas for future manufacturing (Sharfstein, 2022; Tian et al., 2018). These devices not only play a key role in the understanding of biology, physiology, and a variety of pathologies in in vitro studies due to their unique properties, including high sensitivity, selectivity, and non-invasiveness, but also have the potential for brain-computer interfaces and brain repair (Christensen et al., 2022). The challenges in culturing neuronal cells combined with the strong interest in brain/neural-electronic interfaces underscores the need for evaluating and identifying materials used in semiconductor devices that support neural cell growth and differentiation.

In this work, we evaluated the biocompatibility of common microelectronic materials, such as gold (Au), aluminum (Al), titanium nitride (TiN), tantalum nitride (TaN), chromium (Cr), nickel (Ni), nickel/chromium (NiCr) and platinum (Pt), which were deposited onto silicon wafers as single, double, or triple layers of metal thin films by electron-beam physical vapor deposition (EBPVD) or physical vapor deposition (PVD) sputter coating. We choose these metals because some of them have been widely used in the fabrication of biodevices (Au, Al TiN, Pt) (Krauss et al., 2021; Letchumanan et al., 2020; Madhavan et al., 2017; MultiChannelSystems, 2023; Norlin et al., 2005) and compared them to other potential materials that could be used for future biodevice manufacturing (single layer TaN, double layer Ni/Ti, and triple layer NiCr/Ni/Ti). Murine mastocytoma (MST) cells were used as a suspension cell model, and murine NIH

3T3 fibroblasts were used as an adherent cell model to evaluate cell viability, proliferation, cytotoxicity, and morphology on these materials using trypan blue exclusion, MTT, alamarBlue, and LDH assays as well as scanning electron microscopy (SEM). Furthermore, viable cell growth of human induced pluripotent stem cell (iPSC)-derived neural progenitor cells (NPCs) on these materials was evaluated by alamarBlue assay and SEM. iPSC-derived NPC differentiation was evaluated by immunocytochemistry analysis of the neural cell-specific marker, β-tubulin III. Collectively, these studies demonstrate the biocompatibility of silicon chips coated with different metal films (TaN, TiN, Au, Al, Ni/Pt, and NiCr/Ni/Ti) and the feasibility of using these metal surfaces to culture cells, including human iPSC-derived NPCs, and their potential to be used in biomanufacturing devices to interrogate cellular behaviors and biological processes.

2. Materials and Methods

2.1 Preparation of metal-coated silicon chips

We tested a variety of thin films (metal layers) deposited on silicon wafers, which are common microelectronic materials that are integrated into semiconductor devices, including tantalum nitride (nitrogen-poor (TaN P), nitrogen-stoichiometric (TaN S) and nitrogen-rich (TaN R)), titanium nitride (TiN), gold (Au), aluminum (Al), platinum over nickel (Ni/Pt), and titanium over nickel over nickel-chromium (NiCr/Ni/Ti). TaN films deposited onto silicon wafers using a reactive PVD sputtering process in a chamber with argon gas flow and different amounts of nitrogen were provided by NYCREATES (Albany, NY, USA). The remaining thin film depositions were performed using electron beam evaporation. Briefly, silicon wafers were placed into a high-vacuum chamber (~7.5×10^{-5} Torr); which allows the passage of the electrons from the electron gun, and the respective materials were heated until evaporation and deposited at a constant rate on

silicon wafers. These metal-coated silicon wafers were diced using a dicing saw into individual chips (4 mm × 6 mm) for cell culture. All metal surfaces and chips were sterilized by immersion in 70% ethanol for 30 min, followed by exposure to UV light in a biosafety cabinet for 30 min.

2.2 Cell culture

2.2.1 Murine mastocytoma (MST) cells

Murine MST cells previously described (Thacker et al., 2022), which are grown in suspension culture, were maintained in a culture medium consisting of CDM4NS0 (Cytiva, Marlborough, MA, USA), supplemented with 6 mM Gibco™ Glutamax (Thermo Fisher Scientific), 2 g/L Pluronic F-68 (Sigma-Aldrich, St. Louis, MO, USA), and 1:1000 Gibco™ anti-clumping agent (Thermo Fisher Scientific). Cells were cultured in 125 ml Corning polycarbonate Erlenmeyer shake flasks (Thermo Fisher Scientific) on an orbital shaker at 120 rpm in a humidified incubator with 5% CO_2, at 37 °C. Cultures were passaged every 2-3 days with an initial cell seeding density of 2 x 10^5 cells/ml. Murine MST cells were seeded into 24-well plates in the presence of chips coated with the respective metal films (TaN P, TaN S, TaN R, TiN, Au, Al, Ni/Pt, and NiCr/Ni/Ti) and cultured in 1 mL medium in 5% CO_2, at 37 °C and 120 rpm for 5 days. Wells without chips were used as the control. The viable cell density and viability were measured daily using the trypan blue exclusion assay, which is well suited for suspension cultures. 0.4% trypan blue was mixed with an equal volume of cell suspension, followed by counting the number of cells within 3-5 min of mixing using a TC10 Automated Cell Counter (Bio-Rad, Hercules, CA), showing live cell number (unstained cells), total cell number (sum of unstained live cells and dead cells in blue), and cell viability (percentage of live cells divided by total cell number).

2.2.2 Murine NIH 3T3 fibroblasts

Murine NIH 3T3 fibroblasts previously described (Jainchill et al., 1969) were cultured in Gibco™ DMEM (high glucose 4.5 g/L) supplemented with 10% fetal bovine serum, 1% penicillin-streptomycin (10,000 units/mL of penicillin and 10,000 µg/mL of streptomycin) (Thermo Fisher Scientific). Cells were incubated in a 37 °C, 5% CO_2 humidified incubator and subcultured every three days when they were 70-80% confluent. 15,000 cells in 200 µL of medium were seeded into each well of a 96-well plate containing a metal-coated silicon chip (TaN P, TaN S, TaN R, TiN, Au, Al, Ni/Pt, or NiCr/Ni/Ti) or no chip for control wells. Cells were cultured for 48 h in a humidified incubator at 37 °C in 5% CO_2 and then analyzed by alamarBlue, MTT, or LDH assay or SEM.

2.2.3 Human iPSC-derived NPCs

Human iPSC-derived NPCs (Line GIH 161-C4) were provided by the Neural Stem Cell Institute core facility NeuraCell (Rensselaer, NY, USA, https://www.neuracell.org/). After thawing, iPSC-derived NPCs were plated into one well of a laminin 521 (Corning, Bedford, MA)-coated 12-well plate and cultured in 1.5 mL neuronal maintenance medium consisting of Gibco™ advanced DMEM/F12 (Thermo Fisher Scientific, Cat#12644028), 2% MACS® NeuroBrew® -21 with vitamin A (Miltenyi Biotec, Bergisch Gladbach, Germany, Cat#130-093-566), 2 mM L-glutamine and 1% penicillin-streptomycin and maintained in a humidified incubator at 37 °C in 5% CO_2. After 7 days of culture, NPCs were detached using Accutase (MP Biomedicals, Solon, Ohio, USA) per the manufacturer's instructions (0.5 mL incubation at 37 °C and 5% CO_2 for 15 min), counted, and seeded for experiments.

To promote cell adhesion of NPCs, the control well and each metal film-coated silicon chip were coated with laminin 521 at a concentration of 10 µg/mL. Twelve chips per well were placed into a 12-well plate. 500 µL of laminin solution was added to each

well and incubated at 4 °C overnight. After incubation, laminin solution was aspirated, and chips were placed individually into a 96-well plate. 25,000 NPCs in 150 µL of medium were seeded onto the laminin-coated chips (TaN P, TaN S, TaN R, TiN, Au, Al, Ni/Pt, and NiCr/Ni/Ti) in the 96-well plate, using the laminin-coated well without any silicon chips as the control. iPSC-derived NPCs were induced to differentiate into neuronal cells for 10 days. Differentiation medium consisted of BrainPhys™ Neuronal Medium (STEMCELL Technologies, Vancouver, Canada) and 20 ng/mL of brain-derived neurotrophic factor (BDNF) and glial cell line-derived neurotrophic factor (GDNF) (Shenandoah Biotechnology Inc., Warwick, PA, USA). Differentiation medium was changed every other day.

2.3 Cell-metal interaction analysis

2.3.1 MTT assay

NIH 3T3 fibroblast viable cell densities were quantitated using the Roche Cell Proliferation Kit I (MTT) (Millipore Sigma, Burlington, MA, USA). Viable cell density is directly proportional to the purple color resulting from the reduction of the yellow tetrazolium salt MTT to purple formazan crystals. After 48 h of cell culture on different metal-coated silicon chips as described in Section 2.1., 20 µL of MTT solution was added to each well containing 200 µL medium (final MTT concentration 0.5 mg/mL). The 96-well plate was incubated for 4 h in a humidified incubator at 37 °C and 5% CO_2. Subsequently, 100 µL of solubilization buffer was added to each well and the microplate was incubated overnight. The absorbance was measured at a wavelength of 570 nm using a TECAN Infinite M200 microplate reader (TECAN, Morrisville, NC, USA).

2.3.2 alamarBlue assay

Viable cell densities of murine NIH 3T3 fibroblasts and human iPSC-derived NPCs differentiated into neurons were also evaluated by alamarBlue assay in which cells

reduce a blue, weakly fluorescent resazurin into a pink, highly fluorescent resorufin. 200 µL of medium containing 10% (v/v) Invitrogen alamarBlue reagent (Thermo Fisher Scientific) was added to each well, followed by incubation for 2 h at 37 °C and 5% CO_2. 100-µL medium samples were subsequently removed from each well and analyzed using a TECAN Infinite M200 microplate reader. Fluorescence intensity was measured at an excitation wavelength of 545 nm and emission wavelength of 590 nm. Both MTT and alamarBlue assays are widely used to measure cell proliferation and cytotoxicity for adherent cell populations, though both have significant variability (Braun et al., 2018; Hamid et al., 2004; McCutcheon and Fei, n.d.). According to Hamid et al. (2004), based on the toxicity mechanism of the test substances, both assays may produce false positives or false negatives. They showed that MTT can fail to detect the cytotoxicity of compounds such as daunorubicin and trifluoperazine, while this cytotoxicity was evident when performing the alamarBlue assay. In addition, MTT is a destructive assay and cannot be repeated on the same cell population, a limitation when studying the slow growing NPCs derived from limited numbers of iPSCs. By using both assays, we reduced some of the variation in the measurements.

2.3.3 Lactate dehydrogenase (LDH) assay

Cytotoxicity of various metal coatings on silicon chips was assessed by LDH assay for NIH 3T3 fibroblasts grown as described in Section 2.1. LDH is a stable cytoplasmic enzyme that is released upon cell death or other plasma membrane damage and hence, used as a marker for cytotoxicity. Performing LDH assays separates the effects of cytotoxicity from inhibition of proliferation, making it an effective complement to MTT and alamarBlue assays. LDH levels in the cell culture medium were determined using the LDH-Cytox™ Assay Kit (Biolegend, San Diego, CA, USA) according to the manufacturer's instructions. A positive control was generated by adding 20 µL of the

lysis buffer to control cultures (48 hours of growth on tissue culture plastic) and incubating for 30 min in a humidified incubator at 37 °C and 5% CO_2. 100 µL of medium from each sample and control well was transferred to a new, optically clear 96-well plate and 100 µL of the working solution was added. Samples were incubated for 30 min at room temperature protected from light. 50 µL of stop solution was then added, and the absorbance was measured at 490 nm in a TECAN Infinite M200 microplate reader (TECAN, Morrisville, NC, USA).

2.3.4 Immunochemistry analysis and fluorescence microscopy

After culturing in neuronal differentiation medium for 10 days, human iPSC-derived NPCs grown on silicon chips were fixed with 4% paraformaldehyde (Sigma-Aldrich) in Dulbecco's phosphate-buffered saline (DPBS) for 20 min, permeabilized with 0.1% Triton X-100 (Fluka Analytical) for 1h and blocked for 30 min using Invitrogen Cas-Block (Thermo Fisher Scientific). Cells were then incubated with mouse monoclonal primary antibody anti-α-tubulin III (Millipore Sigma) in Cas-Block solution (1:500) overnight at 4 °C. After washing with DPBS three times, samples were incubated with secondary Alexa Fluor 488-conjugated goat anti-mouse antibody (Millipore Sigma) in Cas-Block solution (1:500) at ambient temperature for 1 h. Subsequently, cells were washed three times with DPBS, and DAPI (4′,6-diamidino-2-phenylindole) (1:1000) in DPBS solution was added and incubated at room temperature for 10 min. After washing with DPBS three additional times, samples were mounted using Invitrogen ProLong Gold Antifade (Thermo Fisher Scientific) on microscope slides for imaging. Fluorescence microscopy was performed using an EVOS M7000 Imaging System (Thermo Fisher Scientific) to visualize α-tubulin III using EVOS LIGHT CUBE, GFP 2.0 (Excitation at 470/22 nm/Emission at 525/50 nm) and DAPI-stained nuclei using EVOS Light Cube, DAPI 2.0 (Excitation at 357/44 nm/Emission at 447/60 nm).

2.3.5 Scanning electron microscopy (SEM)

SEM analysis was performed to evaluate cell morphology and distribution on different metal-coated silicon chips two days after seeding for NIH 3T3 fibroblasts and ten days after iPSC-derived NPC differentiation. Cells were washed with DPBS and fixed with 3% glutaraldehyde (Sigma–Aldrich) in 0.1 M phosphate buffer (pH 7.4) (Sigma-Aldrich) and 0.1 M sucrose (Sigma-Aldrich) at room temperature for 2 h. After fixation, samples were dehydrated in a series of graded ethanol concentrations from 25% to 50, 70, 80, 95, 100, and 100% v/v in ethanol/DI water (Thermo Fisher Scientific) for 15 min at each concentration. Samples were subsequently chemically dried with hexamethyldisilane (HMDS) (Sigma-Aldrich) at ethanol to HMDS ratios of 3:1, 1:1, and 1:3 for 15 min each and then in 100% HMDS for 15 min three times. Finally, samples were sputter-coated with iridium, placed on the specimen holder, and imaged with the Zeiss LEO 1550 FE-SEM microscope (Zeiss Leo Electron Microscopy Ltd., Cambridge, UK). 2 kV and magnification of 2000× were used for 3T3 fibroblast samples. For neuronal samples, 3 kV and a magnification of 4500× were used.

2.4 Cytokine quantification by cytokine cytometric bead array.

iPSC-derived NPCs (25,000 cells/well) were grown in differentiation medium for 10 days in laminin-coated control wells (96 well-plate) and on laminin-coated metal thin films, with media changes every other day. At the end of the 10-day period, 200 µL of medium, which had been in contact with the cells for 48 h, was removed from each sample and kept in a -80 °C freezer. Tumor necrosis factor α (TNF-α), interleukin-6 (IL-6), interleukin-10 (IL-10), and interferon-γ (IFN-γ) proteins secreted into culture media were quantitated by Human Inflammatory Cytokine Cytometric Bead Array (CBA) kits (BD Biosciences, San Jose, CA, USA) according to the protocol provided by the manufacturer using flow cytometry on a BD FacsAria II Flow Cytometer.

2.5 Contact angle measurements

Contact angle measurements were conducted using the Video Contact Angle system-VCA Optima (AST Products, Billerica, MA, USA). Using the syringe from the VCA Optima tool, 1 drop (2 μL) of deionized water was deposited on every chip surface and the contact angle was recorded.

2.6 Statistical analysis

Data are represented as mean ± standard deviation. Experiments were repeated at least two times. Statistical analysis was performed using one-way ANOVA and multiple t-tests comparing the different samples to control using GraphPad Prism 9.4.0. software. A p-value < 0.05 was considered statistically significant.

3 Results

3.1 Mastocytoma cell growth and viability in the presence of metal-coated silicon chips

MST cells grew exponentially in all samples (Fig. 1a), including the control cultures and cells exposed to different metal thin film-coated silicon chips (TaN P, TaN S, TaN R, TiN, Au, Al, Ni/Pt, and NiCr/Ni/Ti). After 5 days in culture, the final concentration of MST cells in control wells (in the absence of silicon chips) was $8.89 \pm 2.13 \times 10^6$ cells/mL. MST cell concentrations were slightly lower for wells in the presence of silicon chips; in particular, the silicon chip with the 3-layer NiCr/Ni/Ti thin film deposition, showed the lowest cell concentration ($6.08 \pm 0.70 \times 10^6$ cells/ mL) on day 5. However, there was no significant difference between the viable cell densities on any given day, (Fig. 1a, one-way ANOVA, $p>0.05$).

Further comparison of cell viability showed that MST cells grown in the control wells exhibited greater than 90% viability for 5 days (Fig. 1b). Although in the presence of these metal-coated silicon chips, cell viability slightly decreased, in most cases, cell viability remained above 90%, and the difference between groups was not significant

($p>0.05$) except for the silicon chip with the 3-layer NiCr/Ni/Ti thin film deposition, which showed the lowest cell viability (82.5±0.7%) on day 5 (Fig. 1b). In addition to one-way ANOVA, multiple t-tests were run, and significance was only found between the control and NiCr/Ni/Ti samples on days 4 and 5 (Fig. 1b). Overall, MST cells grew well on these metal-coated silicon chips with viability over 80%, indicating biocompatibility.

3.2 NIH 3T3 fibroblasts proliferation and viable cell growth on metal-coated silicon chips

The viable cell density of NIH 3T3 fibroblasts on the different metal thin film-coated silicon chips (TaN P, TaN S, TaN P, TiN, Au, Al, Ni/Pt, and NiCr/Ni/Ti) was evaluated by MTT and alamarBlue assays after 48 h of cell culture. Both MTT (Fig. 2a) and alamarBlue (Fig. 2b) assays incorporate a redox indicator that changes color or fluorescence in response to cell metabolic activity. Au is a well-known biocompatible material, and NIH 3T3 fibroblasts grown on Au-coated silicon chips for 48 h showed slightly lower cell density by MTT assay compared to the cells grown on the polystyrene control well (Fig. 2a). All three TaN-coated silicon chips (nitrogen-poor, nitrogen-stoichiometric, and nitrogen-rich) supported NIH 3T3 fibroblast growth with cell densities comparable to Au, demonstrating their biocompatibility (Fig. 2a), although the viable cell densities as measured by MTT assay for NIH 3T3 fibroblasts grown on TiN, Al, Ni/Pt, and NiCr/Ni/Ti-coated silicon chip were lower than Au and control (Fig. 2a, one-way ANOVA, $p<0.01$). However, the viable cell density for NIH 3T3 fibroblasts grown on the 3-layer thin film (NiCr/Ni/Ti) was significantly lower than the control (Fig. 2a, one-way ANOVA, $p<0.001$), indicating the possibility of nickel or chromium ion release from this metal-coated silicon chip. alamarBlue assay confirmed the viable cell growth on all these metal-coated silicon chips, showing no significant difference compared to either the polystyrene control or Au (Fig. 2b). LDH results (Fig. 2c) further showed relatively low cell death when culturing on these metal surfaces, comparable to

NIH 3T3 cells grown on the Au-coated silicon chip, confirming little to no cytotoxicity and high relative biocompatibility. Additionally, SEM images of NIH 3T3 fibroblasts grown on different metal thin film-coated silicon chips revealed no prominent changes in cell morphology (Fig. 2d), demonstrating that all metal surfaces support cell attachment and growth of NIH 3T3 fibroblasts.

3.3 Neuronal Differentiation

The viable cell density of human iPSC-derived NPCs grown in differentiation medium for 10 days in laminin-coated control wells and on laminin-coated metal thin films deposited on silicon chips was determined by alamarBlue assay. Fluorescence intensity values and relative cell growth are shown in Fig. 3a and Fig. 3b, respectively. Au- and Al-coated silicon chips exhibited similar iPSC-derived NPC density compared to the polystyrene control well while TiN, Ni/Pt, and NiCr/Ni/Ti-coated silicon chips showed slightly lower cell densities than control. Cell densities were significantly lower in TaN samples, including TaN P, TaN S, and TaN R (one-way ANOVA). Since polystyrene controls are wells in a 96-well plate with a surface of 0.32 cm^2 coated with laminin vs. a chip surface area of 0.24 cm^2 coated with laminin (25,000 NPCs were seeded into all wells with or without chips), a somewhat lower cell number is expected, as seen for the Au-coated chips, but the TaN-coated chips show significantly lower cell densities than the Au-coated chips or polystyrene control wells.

Differentiation of NPCs to neuronal cells was confirmed by SEM (Fig. 4a) and immunocytochemistry (Fig. 4b). SEM images showed that differentiated iPSC-derived NPCs on all metal surfaces exhibited the typical neuronal morphological structure, elongated cells with many neurites extending from the rough and textured cell body (Fig. 4a). Neurites branch and converge at numerous locations, suggestive of a complex neural network. In general, SEM images provided a thorough view of the morphology and structure of neurons, emphasizing the numerous connections between neurons. This

highly branched network was also observed in the respective fluorescence images, where expression of β-tubulin III (green), an early marker of neurons was seen. Nuclear staining with DAPI (blue) shows the total cell population (Fig. 4b).

Furthermore, to study the inflammatory effects of the metal thin films, anti- and pro-inflammatory cytokines (IL-6, IL-10, TNF-α, and IFN-γ) released into media were quantified from neuronal cultures 10 days after iPSC-derived NPC differentiation. (Fig. 5). During inflammation events in the brain, these cytokines can be secreted from neuronal cells (Kronfol, 2000). Here, very low levels of cytokines were measured from all samples, including control cultures. These data suggest these metal thin film-coated silicon chips tested did not illicit an inflammation response.

3.4 Hydrophobicity of TaN surfaces and iPSC-derived NPC growth

The observation that TaN-coated silicon chips supported viable growth of both suspension MST cells and adherent NIH 3T3 fibroblasts at levels comparable to Au-coated ones, but at lower levels for NPC-differentiated neurons promoted us to examine the hydrophobicity of these surfaces. Figure 6a shows that the contact angle on TaN P is over 90 degrees, indicating that the surface is hydrophobic; the hydrophilicity increases as the nitrogen concentration increases, but the nitrogen-rich TaN (TaN R) is still less hydrophilic than gold. To address the effects of surface hydrophobicity, we hypothesized that improving the laminin coating would reduce the impact of the metal surface. After improving laminin coating conditions for the TaN samples, i.e., increasing the amount of laminin solution to 1 mL per well and reducing the number of chips per well during laminin coating from 12 to 9, cell densities increased relative to control (Fig. 6c) compared to chips coated with 500 μL of laminin (Fig. 6b). No difference in viable cell density of iPSC-derived NPCs between the various TaN stoichiometries was observed after improving the laminin coating (Fig. 6c).

4 Discussion

Interest in manufacturing hybrid bio-photonic and electronic devices has been growing significantly in recent years. Gold, platinum, titanium, and titanium nitride have been used in the fabrication of biodevices (Krauss et al., 2021; Madhavan et al., 2017; MultiChannelSystems, 2023; Norlin et al., 2005); however, other materials such as TaN have shown important features with potential utility for biomedical applications. TaN has high corrosion resistance and good electrical, mechanical, and thermal properties, which makes TaN a promising candidate for bio-implantable devices (Alishahi et al., 2016; Hee et al., 2019). The biocompatibility of materials becomes critical for the fabrication and application of biodevices. The interaction of cells with metals can differ depending on the cell type interacting with the metals and what processes are occurring. Furthermore, it is important to carefully evaluate a metal's potential impact on biological systems when combined with other materials. Interfacing these metal films with neuronal cells can help us to understand the feasibility of having this variety of materials for the fabrication of devices for understanding neural biology, treatment of neuropathies, and brain-computer interfacing. In this study, we investigated the biocompatibility of well-known biocompatible materials that are currently used in the fabrication of biodevices with other potential materials for future biomanufacturing.

Several metal thin films deposited onto silicon chips, including TaN fabricated with different nitrogen concentrations, yielding different stoichiometric ratios (poor, stoichiometric, and rich), TiN, Au, Al, double-layer Ni/Pt, and a triple-layer NiCr/Ni/Ti were studied. Different cell types, i.e., murine MST and NIH 3T3 fibroblasts and human iPSC-derived NPCs differentiated into neurons were exposed to these different metals deposited on silicon chips. MST cells grew in suspension in the presence of these chips for 5 days. They grew exponentially with no significant differences between cells grown

in the presence of different metal-coated chips (Fig. 1a). However, cells growing in the presence of NiCr/Ni/Ti thin films showed lower viability on the 4th and 5th day compared to the polystyrene control. We observed the same trend when culturing NIH 3T3 fibroblasts on different metal surfaces. MTT (Fig. 2a) and alamarBlue (Fig. 2b) assays showed similar viable cell densities between the different conditions except for the NiCr/Ni/Ti samples, which showed a slight decrease. NiCr and nickel are two layers that are not directly exposed to the cells (titanium is the top layer, i.e., the exposed one). However, nickel and/or NiCr may be releasing ions that adversely affect cell growth. Previous studies have shown the adverse effects of nickel ions on cell proliferation (Gotman et al., 2013; McLucas et al., 2008), even at concentrations as low as 1.2 μg/mL of Ni^{2+}, increasing lymphocyte proliferation and IL-10 release (Cederbrant et al., 2003). Furthermore, chromium ions can cross the cell membrane, leading to DNA damage, senescence, and apoptosis (Chiu et al., 2010). Interestingly, during neuronal differentiation of the NPCs, no adverse effects were observed in the cultures grown on the NiCr/Ni/Ti-coated chips (Fig. 3), suggesting that the laminin coating might prevent the release of ions from the NiCr/Ni/Ti-coated silicon chips. The potential ion release did not have a great impact on cell proliferation when culturing MST and NIH 3T3 cells, suggesting that very low amounts of Ni and Cr ions might have been released in the medium. Additionally, all the metal thin films supported neuronal differentiation, although TaN samples showed a lower cell density.

Laminin coating is an important factor when differentiating neurons; it enhances NPC adhesion allowing differentiation (Liu et al., 2020). However, laminin is a glycoprotein that has many hydrophilic domains, so it adheres better to hydrophilic surfaces. TaN is more hydrophobic than other surfaces studied in this work (see Fig. 6a and Fig. S1 and Fig. S2). Nitrogen enrichment improved the hydrophilicity of TaN, resulting in a

significant change in cell density between the nitrogen-rich TaN (TaN R) compared to the nitrogen-poor TaN (TaN P). Previous studies showed that the amount of nitrogen can change the wettability of TaN surfaces (Hee et al., 2019; Liao et al., 2023). Upon adding more laminin solution to enhance the coating, the cell density on all three types of TaN-coated silicon chips was relatively similar to the polystyrene control (Fig. 6b). Finally, no inflammatory response was found during neuronal differentiation, indicating that neurons were not affected by the respective metal thin films and that the lower cell densities could be related to the poor adhesion of the laminin coating. Our findings agree with those of previous investigators (Liao et al., 2023; Padilha Fontoura et al., 2021; Turner, 2004), who performed biocompatibility studies on some of the metals presented in this work, including Au, TiN, Pt, or TaN, mainly using fibroblasts or osteoblasts, which are often employed for initial biocompatibility assessments. However, these investigations did not address the suitability of these materials for hiPSC-derived NPC differentiation, and whether combining different metal layers such as the NiCr/Ni/Ti or Ni/Pt stacks can have adverse effects when interfacing with neurons. Moreover, this work demonstrates how the effect of nitrogen content on the wettability of TaN layers becomes an important factor in using coatings like laminin for neuronal differentiation.

5 Conclusions

In summary, metal thin films deposited by EBPVD and PVD sputter coating on silicon chips were studied, analyzing their biocompatibility. To evaluate the biocompatibility in vitro of the thin films, cultures of MST cells, NIH 3T3 fibroblasts, and neuronal differentiation of iPSC-derived neural progenitor cells were performed, evaluating their proliferation, differentiation, and inflammatory responses. Trypan blue staining demonstrated that MST cells proliferate well in the presence of all materials. MTT, LDH, and alamarBlue assays, and SEM analysis indicated that most of the metal

surfaces are cytologically compatible, allowing the attachment and proliferation of NIH 3T3 fibroblasts. Moreover, this analysis, with the addition of immunochemistry and cytokine examination, demonstrated that all these metal thin films support neuronal differentiation. However, there are some limitations to the current study. The exposure time of the metal thin films is a potential concern, as long-term exposure to biological environments can lead to oxidation of these materials and increased ion leaching. Moreover, we did not explore other biological coatings such as Matrigel or fibronectin to promote neuronal cell adhesion, so the interaction of these coatings with the different thin films is unknown. Nonetheless, confirming the feasibility of using the different thin films materials in contact with a range of cultured cells, sets the stage for using these materials for the fabrication of biosensors and neural recording devices and ultimately, exploiting the large-scale production capabilities of microelectronics for scaled-up production of these devices.

Data Availability

Primary research data is available upon request.

Acknowledgments

This project was supported by a grant from the National Science Foundation [ECCS-2134518]. The authors thank Steven Lotz from Neural Stem Cell Institute's core facility NeuraCell for assistance with NPC culture and flow cytometry cytokine measurements, Susan Goderie from Neural Stem Cell Institute for assistance with cell staining protocols and fluorescence imaging, Dr. Runia Roy for assistance with mastocytoma cell culture, and Dr. Xulang Zhang for assistance with initial NIH 3T3 fibroblast culture and alamarBlue assay.

References

Ahnood, A., Chambers, A., Gelmi, A., Yong, K.-T., Kavehei, O., 2023. Semiconducting electrodes for neural interfacing: a review. Chem Soc Rev 52, 1491–1518. https://doi.org/10.1039/D2CS00830K

Alishahi, M., Mahboubi, F., Mousavi Khoie, S.M., Aparicio, M., Lopez-Elvira, E., Méndez, J., Gago, R., 2016. Structural properties and corrosion resistance of tantalum nitride coatings produced by reactive DC magnetron sputtering. RSC Adv 6, 89061–89072. https://doi.org/10.1039/C6RA17869C

Anderson, J.M., 2019. Biocompatibility and Bioresponse to Biomaterials, in: Principles of Regenerative Medicine. Elsevier, pp. 675–694. https://doi.org/10.1016/B978-0-12-809880-6.00039-4

Beck, H., Boden, W.E., Patibandla, S., Kireyev, D., Gupta, V., Campagna, F., Cain, M.E., Marine, J.E., 2010. 50th Anniversary of the First Successful Permanent Pacemaker Implantation in the United States: Historical Review and Future Directions. Am J Cardiol 106, 810–818. https://doi.org/10.1016/j.amjcard.2010.04.043

Braun, K., Stürzel, C.M., Biskupek, J., Kaiser, U., Kirchhoff, F., Lindén, M., 2018. Comparison of different cytotoxicity assays for in vitro evaluation of mesoporous silica nanoparticles. Toxicology in Vitro 52, 214–221. https://doi.org/10.1016/j.tiv.2018.06.019

Cederbrant, K., Anderson, C., Andersson, T., Marcusson-Ståhl, M., Hultman, P., 2003. Cytokine Production, Lymphocyte Proliferation and T-Cell Receptor Vβ Expression in Primary Peripheral Blood Mononuclear Cell Cultures from Nickel-Allergic Individuals. Int Arch Allergy Immunol 132, 373–379. https://doi.org/10.1159/000074905

Chiu, A., Shi, X.L., Lee, W.K.P., Hill, R., Wakeman, T.P., Katz, A., Xu, B., Dalal, N.S., Robertson, J.D., Chen, C., Chiu, N., Donehower, L., 2010. Review of Chromium (VI) Apoptosis, Cell-Cycle-Arrest, and Carcinogenesis. Journal of Environmental Science and Health, Part C 28, 188–230. https://doi.org/10.1080/10590501.2010.504980

Christensen, D. V, Dittmann, R., Linares-Barranco, B., Sebastian, A., Le Gallo, M., Redaelli, A., Slesazeck, S., Mikolajick, T., Spiga, S., Menzel, S., Valov, I., Milano, G., Ricciardi, C., Liang, S.-J., Miao, F., Lanza, M., Quill, T.J., Keene, S.T., Salleo, A., Grollier, J., Marković, D., Mizrahi, A., Yao, P., Yang, J.J., Indiveri, G., Strachan, J.P., Datta, S., Vianello, E., Valentian, A., Feldmann, J., Li, X., Pernice, W.H.P., Bhaskaran, H., Furber, S., Neftci, E., Scherr, F., Maass, W., Ramaswamy, S., Tapson, J., Panda, P., Kim, Y., Tanaka, G., Thorpe, S., Bartolozzi, C., Cleland, T.A., Posch, C., Liu, S., Panuccio, G., Mahmud, M., Mazumder, A.N., Hosseini, M., Mohsenin, T., Donati, E., Tolu, S., Galeazzi, R., Christensen, M.E., Holm, S., Ielmini, D., Pryds, N., 2022. 2022 roadmap on neuromorphic computing and engineering. Neuromorphic Computing and Engineering 2, 022501. https://doi.org/10.1088/2634-4386/ac4a83

Clark, G.M., 2006. The multiple-channel cochlear implant: the interface between sound and the central nervous system for hearing, speech, and language in deaf people—a personal perspective. Philosophical Transactions of the Royal Society B: Biological Sciences 361, 791–810. https://doi.org/10.1098/rstb.2005.1782

Fattahi, P., Yang, G., Kim, G., Abidian, M.R., 2014. A Review of Organic and Inorganic Biomaterials for Neural Interfaces. Advanced Materials 26, 1846–1885. https://doi.org/10.1002/adma.201304496

Gimsa, J., Habel, B., Schreiber, U., Rienen, U. van, Strauss, U., Gimsa, U., 2005. Choosing electrodes for deep brain stimulation experiments–electrochemical considerations. J Neurosci Methods 142, 251–265. https://doi.org/10.1016/j.jneumeth.2004.09.001

Gotman, I., Ben-David, D., Unger, R.E., Böse, T., Gutmanas, E.Y., Kirkpatrick, C.J., 2013. Mesenchymal stem cell proliferation and differentiation on load-bearing trabecular Nitinol scaffolds. Acta Biomater 9, 8440–8448. https://doi.org/10.1016/j.actbio.2013.05.030

Hamid, R., Rotshteyn, Y., Rabadi, L., Parikh, R., Bullock, P., 2004. Comparison of alamar blue and MTT assays for high through-put screening. Toxicology in Vitro 18, 703–710. https://doi.org/10.1016/j.tiv.2004.03.012

Hee, A.C., Zhao, Y., Jamali, S.S., Bendavid, A., Martin, P.J., Guo, H., 2019. Characterization of tantalum and tantalum nitride films on Ti6Al4V substrate prepared by filtered cathodic vacuum arc deposition for biomedical applications. Surf Coat Technol 365, 24–32. https://doi.org/10.1016/j.surfcoat.2018.05.007

Jainchill, J.L., Aaronson, S.A., Todaro, G.J., 1969. Murine Sarcoma and Leukemia Viruses: Assay Using Clonal Lines of Contact-Inhibited Mouse Cells. J Virol 4, 549–553. https://doi.org/10.1128/jvi.4.5.549-553.1969

Krauss, J.K., Lipsman, N., Aziz, T., Boutet, A., Brown, P., Chang, J.W., Davidson, B., Grill, W.M., Hariz, M.I., Horn, A., Schulder, M., Mammis, A., Tass, P.A., Volkmann, J., Lozano, A.M., 2021. Technology of deep brain stimulation: current status and future directions. Nat Rev Neurol 17, 75–87. https://doi.org/10.1038/s41582-020-00426-z

Kronfol, Z., 2000. Cytokines and the Brain: Implications for Clinical Psychiatry. American Journal of Psychiatry 157, 683–694. https://doi.org/10.1176/appi.ajp.157.5.683

Letchumanan, I., Md Arshad, M.K., Gopinath, S.C.B., Rajapaksha, R.D.A.A., Balakrishnan, S.R., 2020. Comparative Analysis on Dielectric Gold and Aluminium Triangular Junctions: Impact of Ionic Strength and Background Electrolyte by pH Variations. Sci Rep 10, 6783. https://doi.org/10.1038/s41598-020-63831-w

LI, Weijia, Zhou, J., Xu, Y., 2015. Study of the in vitro cytotoxicity testing of medical devices. Biomed Rep 3, 617–620. https://doi.org/10.3892/br.2015.481

Liao, S., Yang, L., Song, Z., Zhou, Z., Zhang, Q., Yang, C., Zheng, J., 2023. Effect of nitrogen content on the mechanical and biological properties of tantalum nitride coatings. Surf Coat Technol 464, 129544. https://doi.org/10.1016/j.surfcoat.2023.129544

Liu, D., Pavathuparambil Abdul Manaph, N., Al-Hawwas, M., Bobrovskaya, L., Xiong, L.-L., Zhou, X.-F., 2020. Coating Materials for Neural Stem/Progenitor Cell Culture and Differentiation. Stem Cells Dev 29, 463–474. https://doi.org/10.1089/scd.2019.0288

Madhavan, M., Mulpuru, S.K., McLeod, C.J., Cha, Y.-M., Friedman, P.A., 2017. Advances and Future Directions in Cardiac Pacemakers. J Am Coll Cardiol 69, 211–235. https://doi.org/10.1016/j.jacc.2016.10.064

McCutcheon, K., Fei, D., n.d. Comparing Quantitative Viability Bioassays: An Evaluation of MTT, alamarBlue™, and Guava® ViaCount® Methods [WWW Document]. URL https://www.sigmaaldrich.com/US/en/technical-documents/technical-article/cell-culture-and-cell-culture-analysis/cell-counting-and-health-analysis/an-evaluation-of-mtt-alamarblue-and-guava-viacount-methods (accessed 9.25.23).

McLucas, E., Rochev, Y., Carroll, W.M., Smith, T.J., 2008. Analysis of the effects of surface treatments on nickel release from nitinol wires and their impact on candidate gene expression in endothelial cells. J Mater Sci Mater Med 19, 975–980. https://doi.org/10.1007/s10856-006-0087-9

MultiChannelSystems, 2023. Microelectrode arrays [WWW Document]. URL https://www.multichannelsystems.com/products/microelectrode-arrays (accessed 6.11.23).

Norlin, A., Pan, J., Leygraf, C., 2005. Investigation of Electrochemical Behavior of Stimulation/Sensing Materials for Pacemaker Electrode Applications. J Electrochem Soc 152, J7. https://doi.org/10.1149/1.1842092

Padilha Fontoura, C., Ló Bertele, P., Machado Rodrigues, M., Elisa Dotta Maddalozzo, A., Frassini, R., Silvestrin Celi Garcia, C., Tomaz Martins, S., Crespo, J. da S., Figueroa, C.A., Roesch-Ely, M., Aguzzoli, C., 2021. Comparative Study of Physicochemical Properties and Biocompatibility (L929 and MG63 Cells) of TiN Coatings Obtained by Plasma Nitriding and Thin Film Deposition. ACS Biomater Sci Eng 7, 3683–3695. https://doi.org/10.1021/acsbiomaterials.1c00393

Perlmutter, J.S., Mink, J.W., 2006. DEEP BRAIN STIMULATION. Annu Rev Neurosci 29, 229–257. https://doi.org/10.1146/annurev.neuro.29.051605.112824

Roehm, N.W., Rodgers, G.H., Hatfield, S.M., Glasebrook, A.L., 1991. An improved colorimetric assay for cell proliferation and viability utilizing the tetrazolium salt XTT. J Immunol Methods 142, 257–265. https://doi.org/10.1016/0022-1759(91)90114-U

Salerno, A., Guarnieri, D., Iannone, M., Zeppetelli, S., Di Maio, E., Iannace, S., Netti, P.A., 2009. Engineered μ-bimodal poly(ε-caprolactone) porous scaffold for enhanced hMSC colonization and proliferation. Acta Biomater 5, 1082–1093. https://doi.org/10.1016/j.actbio.2008.10.012

Sharfstein, S.T., 2022. Bio-hybrid electronic and photonic devices. Exp Biol Med 247, 2128–2141. https://doi.org/10.1177/15353702221144087

Thacker, B.E., Thorne, K.J., Cartwright, C., Park, J., Glass, K., Chea, A., Kellman, B.P., Lewis, N.E., Wang, Z., Di Nardo, A., Sharfstein, S.T., Jeske, W., Walenga, J., Hogwood, J., Gray, E., Mulloy, B., Esko, J.D., Glass, C.A., 2022. Multiplex genome editing of mammalian cells for producing recombinant heparin. Metab Eng 70, 155–165. https://doi.org/10.1016/j.ymben.2022.01.002

Tian, B., Xu, S., Rogers, J.A., Cestellos-Blanco, S., Yang, P., Carvalho-de-Souza, J.L., Bezanilla, F., Liu, J., Bao, Z., Hjort, M., Cao, Y., Melosh, N., Lanzani, G., Benfenati, F., Galli, G., Gygi, F., Kautz, R., Gorodetsky, A.A., Kim, S.S., Lu, T.K., Anikeeva, P., Cifra, M., Krivosudský, O., Havelka, D., Jiang, Y., 2018. Roadmap on semiconductor–cell biointerfaces. Phys Biol 15, 031002. https://doi.org/10.1088/1478-3975/aa9f34

Turner, N., 2004. An in vitro model to evaluate cell adhesion to metals used in implantation shows significant differences between palladium and gold or platinum. Cell Biol Int 28, 541–547. https://doi.org/10.1016/j.cellbi.2004.04.009

Wang, L., Jiang, X., Ji, Y., Bai, R., Zhao, Y., Wu, X., Chen, C., 2013. Surface chemistry of gold nanorods: origin of cell membrane damage and cytotoxicity. Nanoscale 5, 8384. https://doi.org/10.1039/c3nr01626a

Wilson, B.S., Dorman, M.F., 2008. Cochlear implants: A remarkable past and a brilliant future. Hear Res 242, 3–21. https://doi.org/10.1016/j.heares.2008.06.005

Yue, L., Weiland, J.D., Roska, B., Humayun, M.S., 2016. Retinal stimulation strategies to restore vision: Fundamentals and systems. Prog Retin Eye Res 53, 21–47. https://doi.org/10.1016/j.preteyeres.2016.05.002

Figure Legends

Fig. 1. Evaluation of biocompatibility of metal-coated silicon chips using suspension-cultured MST cells by trypan blue exclusion assay. (a) Viable cell density for 5 days of culture in the presence of silicon chips coated with different metal thin films (TaN P, TaN S, TaN R, TiN, Au, Al, Ni/Pt, and NiCr/Ni/Ti,). (b) Viability of MST cells cultured for 5 days in the presence of different metal-coated silicon chips. ns, not significant. * $p < 0.05$. N=3.

Fig. 2. Evaluation of biocompatibility of silicon chips coated with different metal thin films (TaN P, TaN S, TaN R, TiN, Au, Al, Ni/Pt, and NiCr/Ni/Ti) using NIH 3T3 fibroblasts grown on them for 48 h. (a) MTT assay. (b) alamarBlue assay. (c) LDH assay. (d) Top view of SEM images showing the morphology of NIH 3T3 fibroblasts after 2 days of culture on a variety of metal thin films deposited on silicon chips. Scale bar = 20 μm. ** $p<0.01$; **** $p<0.0001$. N=3.

Fig. 3. Viable cell density of human iPSC-derived NPCs grown on laminin-coated metal thin films on silicon chips (TaN P, TaN S, TaN R, TiN, Au, Al, Ni/Pt, and NiCr/Ni/Ti) and induced to differentiate for 10 days. (a) Fluorescence intensity assessed by alamarBlue assay. (b) Relative cell growth normalized by the fluorescence intensity of the laminin-coated polystyrene control well. * $p<0.05$; ** $p<0.01$; *** $p<0.001$; **** $p<0.0001$. N=3. Note that the surface area of a chip (0.24 cm^2) is less than the surface area of the control well (0.32 cm^2), and therefore, a lower relative cell density is expected.

Fig. 4. (a) SEM images showing the morphology of neurons after 10 days of differentiation from human iPSC-derived NPCs on laminin-coated metal thin films on silicon chips (TaN P, TaN S, TaN R, TiN, Au, Al, Ni/Pt, and NiCr/Ni/Ti). Scale bar = 10 μm. (b) Fluorescence images showing expression of neuronal marker β-tubulin III in human iPSC-derived NPCs after 10 days of differentiation on laminin-coated metal thin films on silicon chips (TaN P, TaN S, TaN R, TiN, Au, Al, Ni/Pt, and NiCr/Ni/Ti). Green: β-tubulin III. Blue: DAPI-stained nuclei. Scale bar = 50 μm.

Fig. 5. Cytokine release by human iPSC-derived NPCs after 10 days of differentiation on different laminin-coated metal thin films on silicon chips (TaN P, TaN S, TaN R, TiN, Au, Al, Ni/Pt, and NiCr/Ni/Ti). Results are expressed as the mean of a fluorescence intensity, which is proportional to the concentration of the respective cytokine released into the culture media. N = 3.

Fig. 6. Wetting properties of and cell growth on different TaN-coated silicon chips. (a) Contact angle of TaN thin films (TaN P, TaN S, and TaN R) compared to the gold thin film. (b, c) Viable cell density of human iPSC-derived NPCs grown on laminin-coated TaN thin film on silicon chips and induced to differentiation for 10 days assessed by alamarBlue assay (b) with 500 μL of laminin coating solution or (c) with 1 mL laminin coating solution per well in a 12 well-plate. Laminin-coated cell culture polystyrene wells were used as the control. * $p<0.05$; ** $p<0.01$. N=3.

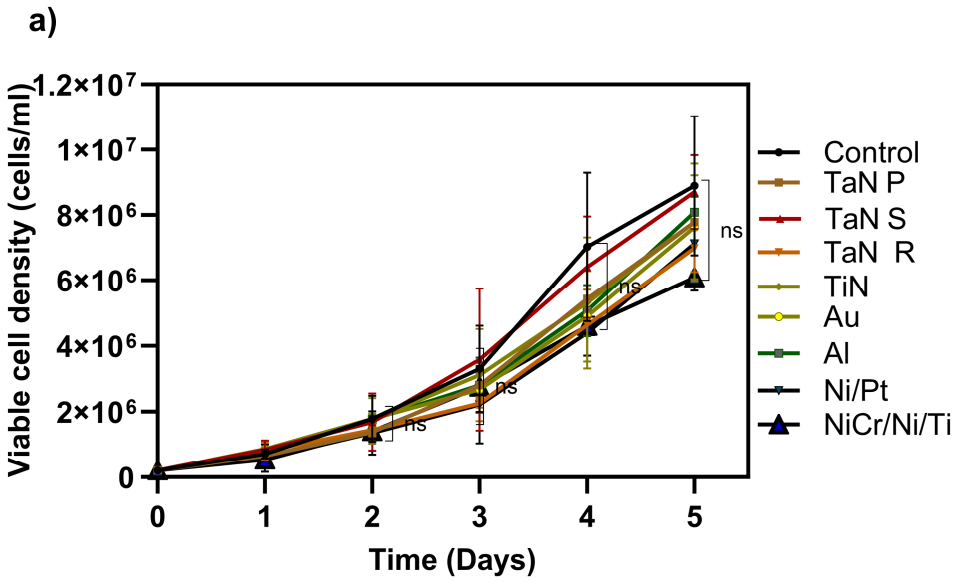
a)
Viable cell density (cells/ml)
1.2×10^7
1×10^7
8×10^6
6×10^6
4×10^6
2×10^6
0
0
1
2
3
4
5
Time (Days)
ns
ns
ns
ns
Control
TaN P
TaN S
TaN R
TiN
Au
Al
Ni/Pt
NiCr/Ni/Ti

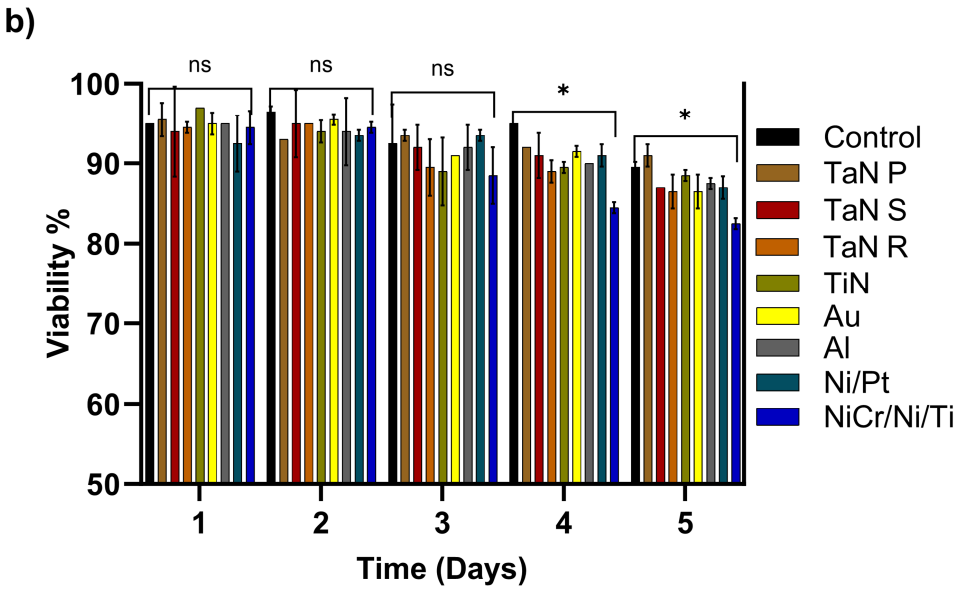
b)
Viability %
100
90
80
70
60
50
1
2
3
4
5
Time (Days)
ns
ns
ns
*
*
Control
TaN P
TaN S
TaN R
TiN
Au
Al
Ni/Pt
NiCr/Ni/Ti

a)

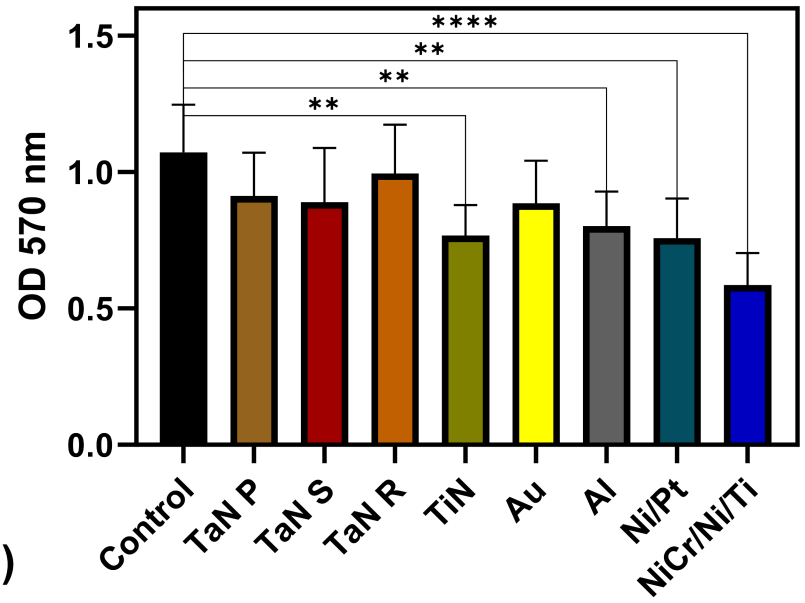
OD 570 nm
1.5
1.0
0.5
0.0
****
**
**
**
Control
TaN P
TaN S
TaN R
TiN
Au
Al
Ni/Pt
NiCr/Ni/Ti

b)

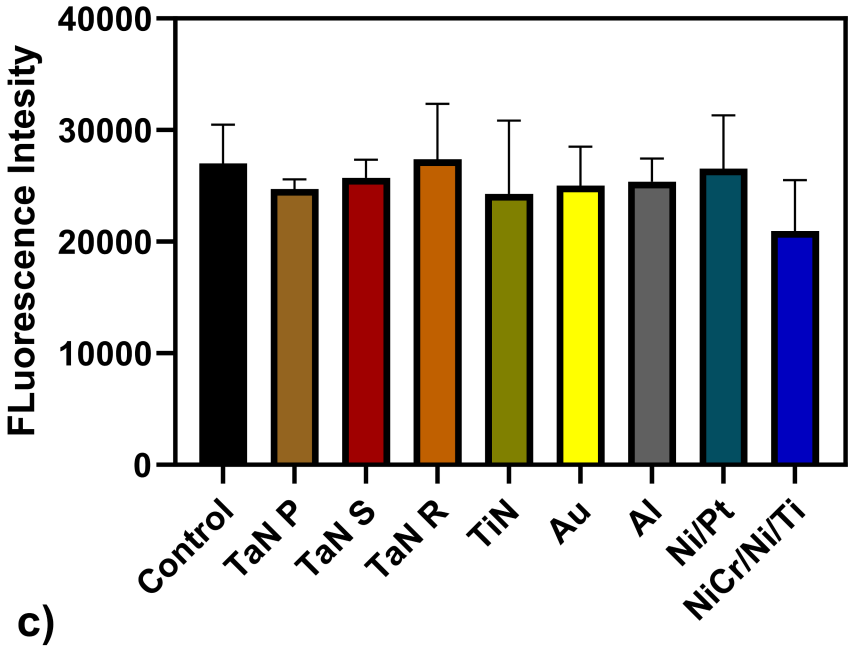
FLuorescence Intesity
40000
30000
20000
10000
0
Control
TaN P
TaN S
TaN R
TiN
Au
Al
Ni/Pt
NiCr/Ni/Ti

c)

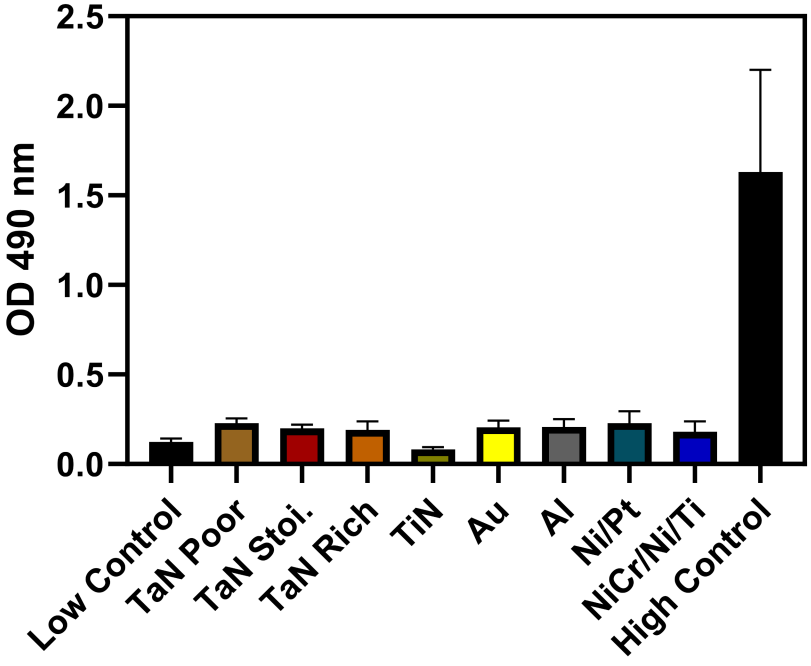
OD 490 nm
2.5
2.0
1.5
1.0
0.5
0.0
Low Control
TaN Poor
TaN Stoi.
TaN Rich
TiN
Au
Al
Ni/Pt
NiCr/Ni/Ti
High Control

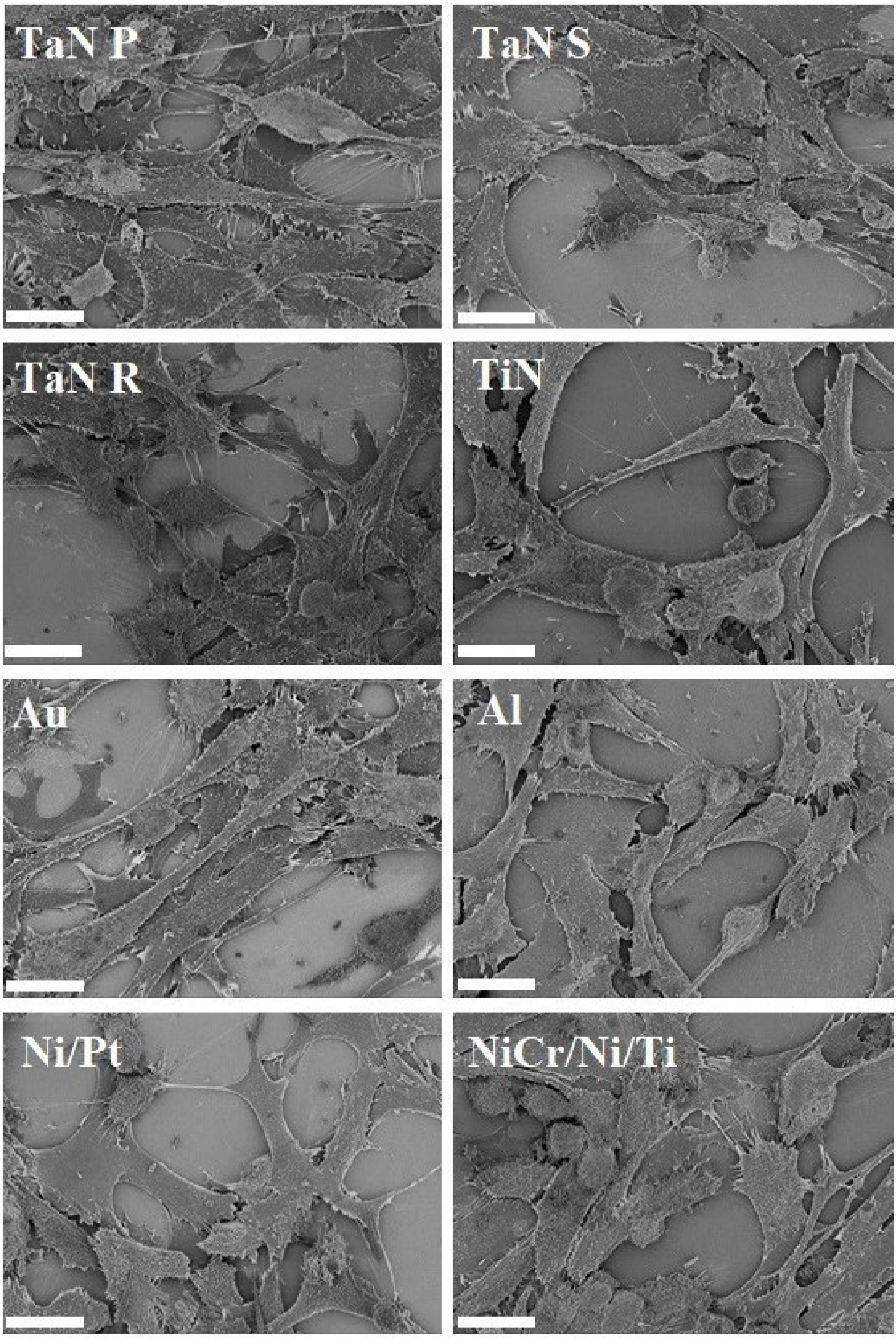
TaN P
TaN S
TaN R
TiN
Au
Al
Ni/Pt
NiCr/Ni/Ti

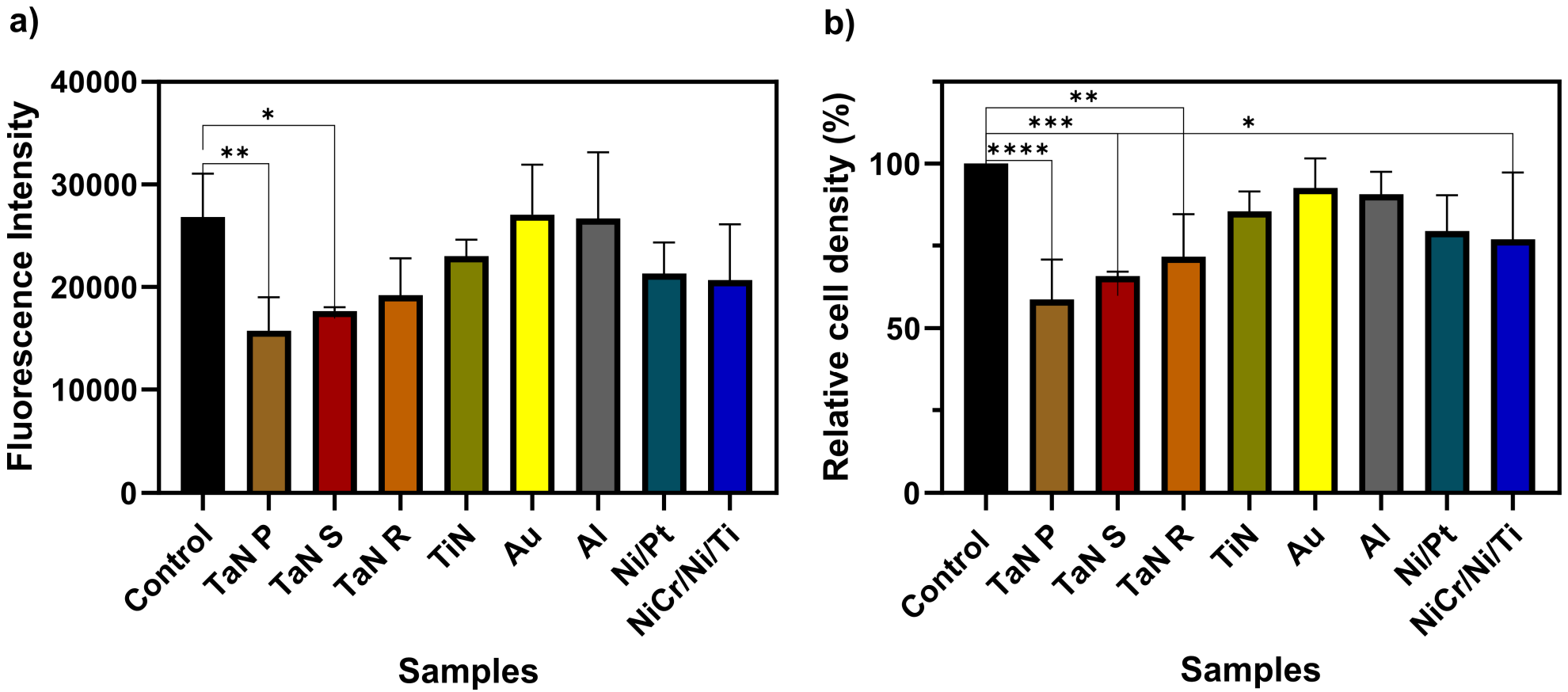
a)
Fluorescence Intensity
40000
30000
20000
10000
0
**
*
Control
TaN P
TaN S
TaN R
TiN
Au
Al
Ni/Pt
NiCr/Ni/Ti
Samples
b)
Relative cell density (%)
100
50
0
**
***
****
*
Control
TaN P
TaN S
TaN R
TiN
Au
Al
Ni/Pt
NiCr/Ni/Ti
Samples

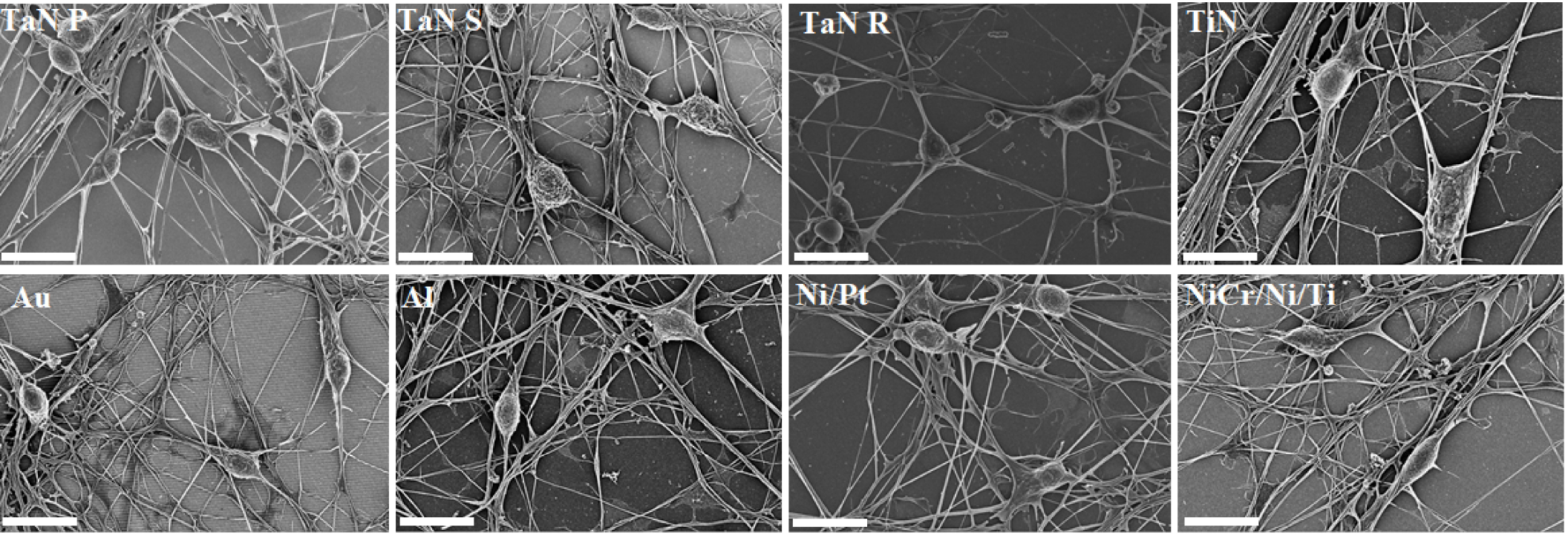
TaN P
TaN S
TaN R
TiN
Au
Al
Ni/Pt
NiCr/Ni/Ti

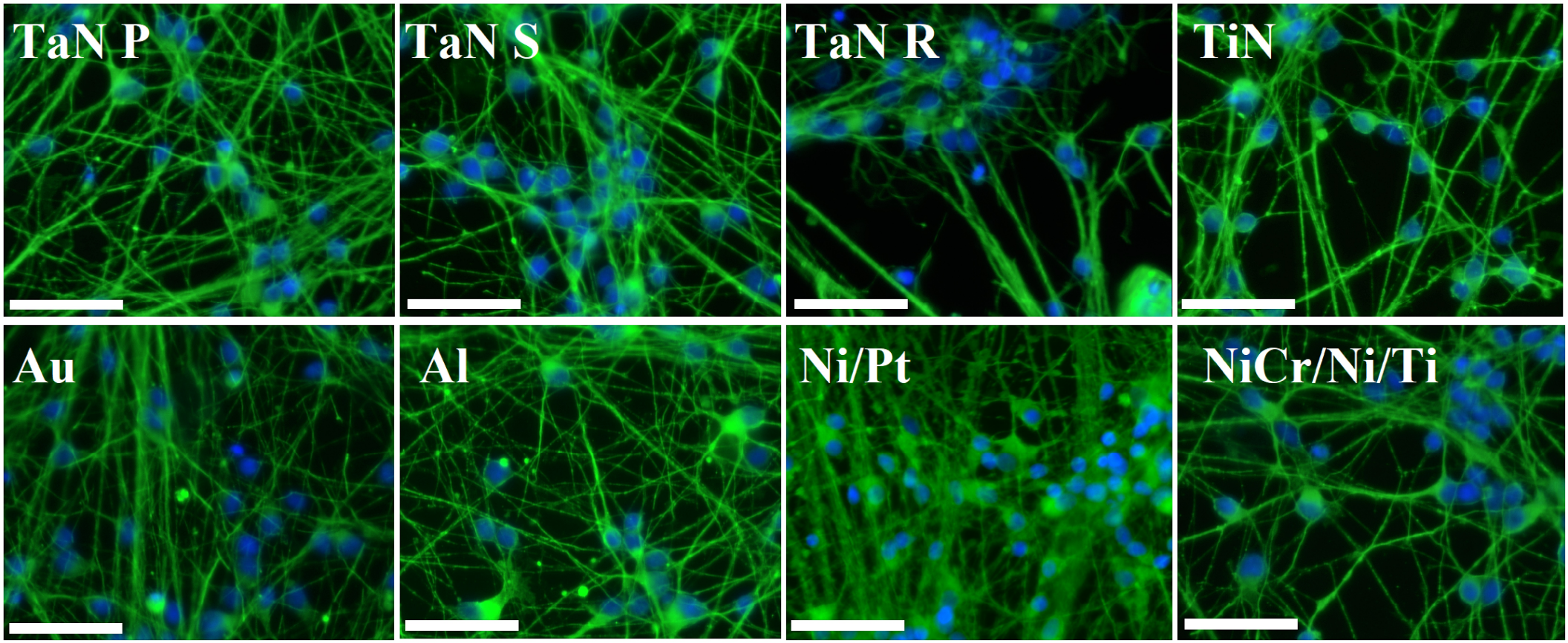
TaN P
TaN S
TaN R
TiN
Au
Al
Ni/Pt
NiCr/Ni/Ti

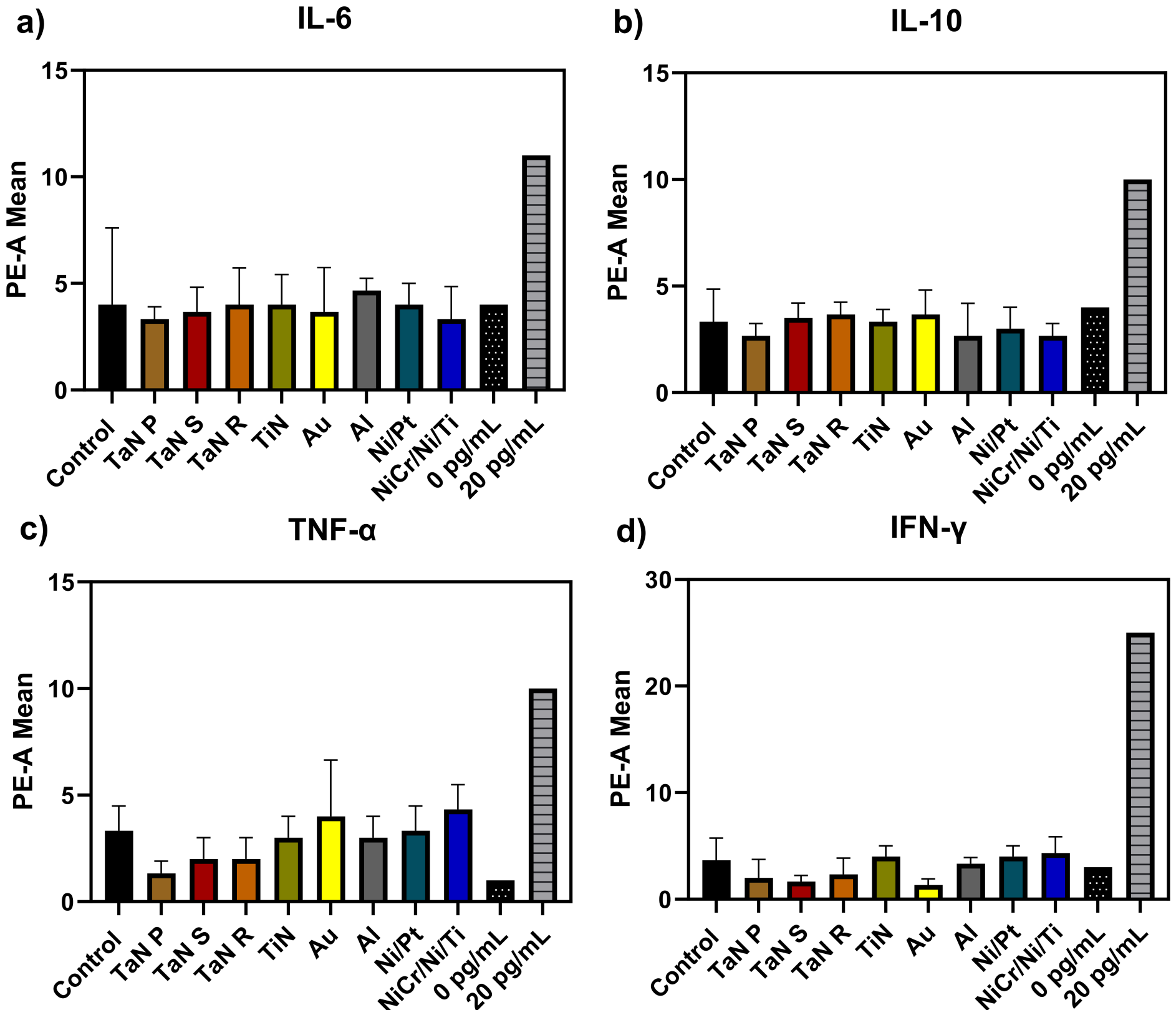
a)
IL-6
PE-A Mean
15
10
5
0
Control
TaN P
TaN S
TaN R
TiN
Au
Al
Ni/Pt
NiCr/Ni/Ti
0 pg/mL
20 pg/mL
b)
IL-10
PE-A Mean
15
10
5
0
Control
TaN P
TaN S
TaN R
TiN
Au
Al
Ni/Pt
NiCr/Ni/Ti
0 pg/mL
20 pg/mL
c)
TNF-α
PE-A Mean
15
10
5
0
Control
TaN P
TaN S
TaN R
TiN
Au
Al
Ni/Pt
NiCr/Ni/Ti
0 pg/mL
20 pg/mL
d)
IFN-γ
PE-A Mean
30
20
10
0
Control
TaN P
TaN S
TaN R
TiN
Au
Al
Ni/Pt
NiCr/Ni/Ti
0 pg/mL
20 pg/mL

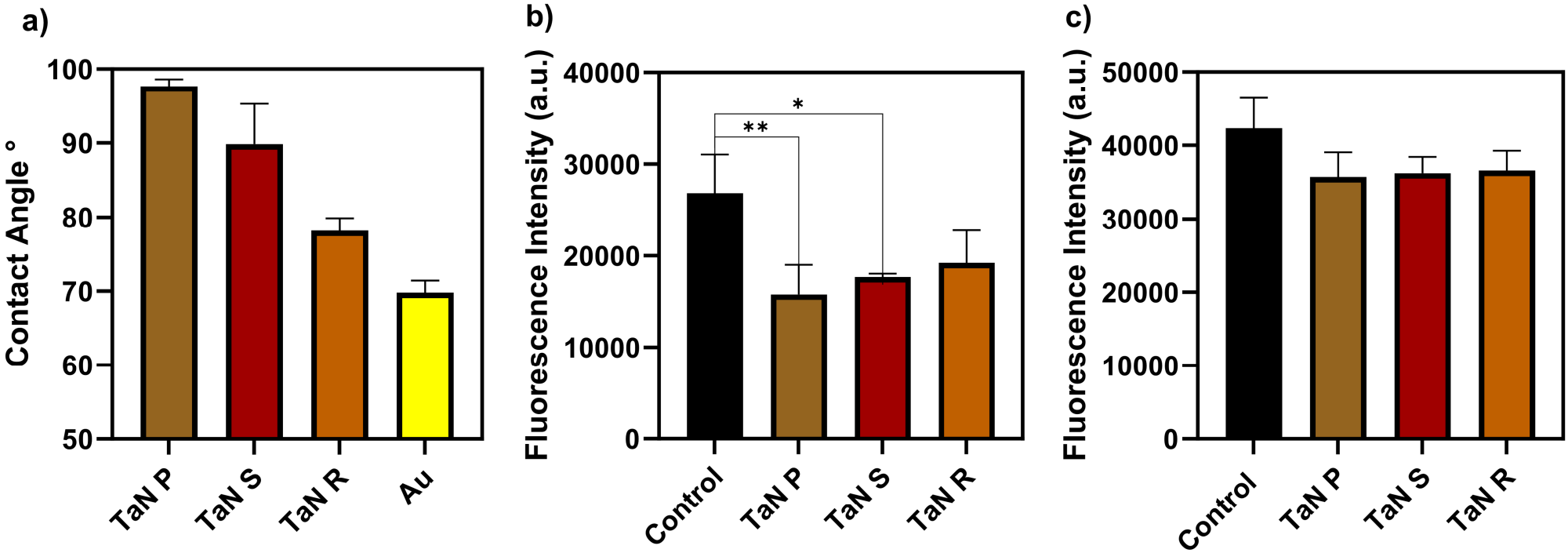
a)
Contact Angle °
100
90
80
70
60
50
TaN P
TaN S
TaN R
Au
b)
Fluorescence Intensity (a.u.)
40000
30000
20000
10000
0
**
*
Control
TaN P
TaN S
TaN R
c)
Fluorescence Intensity (a.u.)
50000
40000
30000
20000
10000
0
Control
TaN P
TaN S
TaN R

Supplementary Information

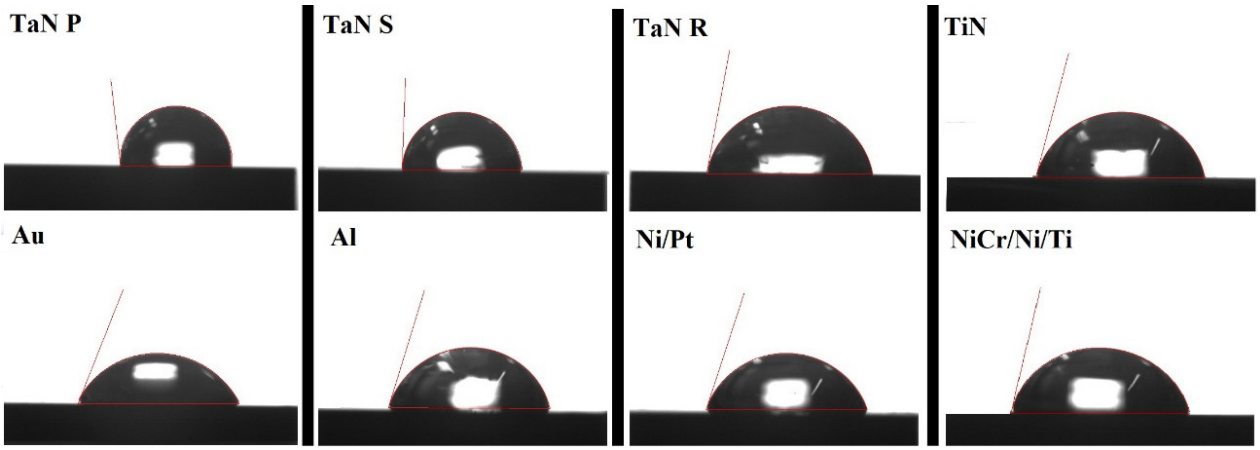

Figure S1. Images of contact angle comparisons between the different metal thin film-coated silicon chips (TaN P, TaN S, TaN R, TiN, Au, Al, Ni/Pt, and NiCr/Ni/Ti).

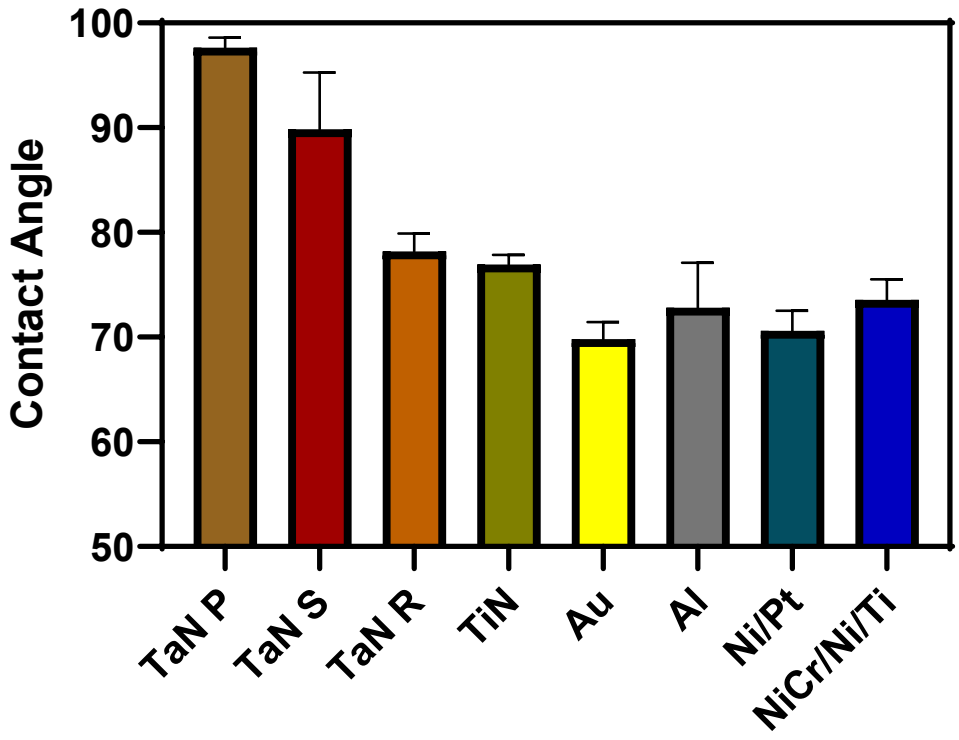

Figure S2. Contact angles of the different metal thin film-coated silicon chips. N=3